DATA DRIVEN MODEL FOR ROOFTOP EXCESS ELECTRICITY GENERATION

Yohei Kiguchi[1], Yeonsook Heo[1,2], Ruchi Choudhary[1]
[1]Energy Efficient Cities Initiative, University of Cambridge, United Kingdom
[2]Department of Architecture, University of Cambridge, Cambridge, United Kingdom

ABSTRACT

Large-scale rooftop PV deployment generates significant amounts of excess electricity (the difference between real-time PV generation and on-site consumption). Accurate forecasting of excess electricity generation becomes important for energy traders participating in a liberalised electricity market in order to avoid penalties imposed by the market in case of imbalance between actual and predicted values. This paper proposes a data-driven Gaussian Process model for forecasting excess-generation of electricity. An illustrative study, with a-year long dataset from 287 households, is used to derive the forecasting model. Results show that a-year-long data from 18 households is sufficient for accurate prediction of excess generation across a uniform geographic and socio-economic setting.

INTRODUCTION

Residential PV systems make up the dominant share of solar energy deployment worldwide, and they are anticipated to remain the dominant driver for PV generation deployment: around 60% in 2010, and 40% in 2050 among the four market segments (residential, commercial, utility-scale, and off-grid) (IEA, 2010).

In the residential sector, there is usually a poor correlation between load and generation; more energy is generated during daytime, whilst consumption is highest in the morning and in the evening hours (see Figure 1). Excess-generation is the result of this mismatch between the timing of generation and consumption. Energy traders participating in liberalised markets aggregate the excess energy produced by many rooftop installations to sell it. They need to notify the amount of energy that they can provide in advance and in case of imbalance between the bid and the actual amount of energy they are subject to penalties and/or loss of revenues (Pinson et al., 2007). In this scenario, accurate excess-generation forecasting becomes crucial to optimise the revenues of the traders, and thus encourage the installation of rooftop PV systems.

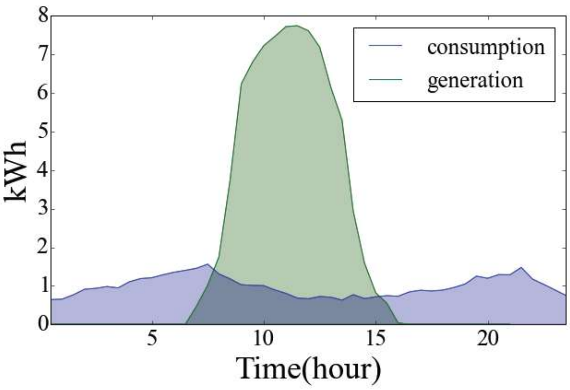

Figure 1: Typical daily energy usage of a PV installed household. Excess-generation is a result of a mismatch between the timing of PV generation and consumption.

Accurate prediction of excess generation is also essential for grid operators, since inaccurate predictions of excess electricity into the grid from several thousands of PV systems, scattered geographically, can be challenging for grid stability (Denholm et al., 2007).

PV generation, on-site consumption, and therefore, excess-generation is measurable in real-time through a single device – the smart meter. Indeed, many countries are showing a strong commitment to support large-scale smart-metering programs, with the aim of better real-time management of electricity flows through the grid. In 2009, the European Commission Directive required that 80% of EU households have smart meters installed by 2020. This is likely to result in an exponentially increasing available datasets, which will be invaluable for predicting future excess-generation using data-driven methods.

Excess-generation is essentially the result of the difference between real-time PV generation and on-site load consumption. Individual models for predicting PV generation and on-site consumption have been researched extensively. However, to the author's knowledge, no model exists that integrated generation and consumption uniquely for the goal of quantifying excess generation. This paper compares the forecasting accuracy of an integrated excess-generation model against the more traditional decoupled approach and thereby examines the necessity of an integrated excess-generation model.

Next section provides an overview of relevant existing energy demand and PV generation models. The next section describes the dataset of an illustrative study and proposes an integrated modelling procedure for predicting excess-generation. Finally, prediction results of the proposed model are compared against ‘decoupled model (model for PV generation minus load consumption). The conclusion explains two key findings and scheduled future work.

LITERATURE REVIEW

Excess-generation can be considered as a function of PV generation and on-site load consumption. PV generation and residential consumption models are useful in pre-screening important features for excess-generation modelling as explanatory variables/inputs. In this section, recent studies in these fields are reviewed in order to identify key variables for excess-generation modelling.

PV Generation Models

Models for predicting PV generation are categorised into engineering (physical) models and statistical time-series models. An engineering model involves a physics-based model of PV panels, which converts solar irradiance to output power. Various simulation tools are currently available to perform PV simulation, e.g., TRNSYS; RETScreen; PVSIM; PVFORM; PVNet; and so on. The *RETScreen Photovoltaic Project Model* (Clean Energy Decision Support Centre., 2004) mainly utilises site-specific weather information (especially insolation), as well as configuration of a PV system. TRNSYS is used for dynamic simulation with modelling of solar radiation, PV array output, and inverter output (Jayanta et al., 2007).

On the other hand, statistical models predict future PV output by computing the trend of the output based on present and past samples of PV generation. Meteorological parameters, including temperature, clearness, dust, and relative humidity, are frequently considered as explanatory variables in such models (Türk et al., 1999). For example, (Long et al. 2014) survey multiple features (as inputs) that can improve accuracy of daily PV generation based on two years’ data collected in Macau on four types of machine learning models: Artificial Neural Network, Support Vector Machine, *k*-nearest neighbour, and the multivariate linear regression. Parameters shown to be important across all the four models include maximum air temperature, daily mean air temperature, insolation, wind-speed, precipitation and day-before PV generation.

(Huang et al., 2010) contrasted the performance of an engineering (diode) model and a statistical model (Neural Network) in a case study of a 1 MW PV station. The performance difference is measured by nRMSE. The paper finds that the statistical model using temperature, cloud coefficient, irradiance, humidity, and the position of sun as inputs shows better performance than a diode physical model.

On-site Load Models

Various technical studies for modelling residential sector energy consumption are relevant for identifying key features that influence household electricity consumption patterns during daytime hours (defined as the hours during which excess-generation is possible).

One study (Parti., 1980) identifies important features influencing consumption corresponding to end-use groups: the number of occupants, electricity price, household income, floor area, and heating/cooling per unit area.

(Shimoda et al., 2004) developed a residential end-use energy consumption model for the city of Osaka, Japan. In this model, households are rated based on the number of family members, appliance ownership levels, and appliance ratings. (Shimoda et al., 2007) simulated electricity consumption used by each appliance at five-minute intervals, according to the occupants’ energy-usage activity. These studies yield valuable conclusions for end-use electricity consumption patterns. First, electricity consumption depends more on the number of family members in a household than on the total floor area of the house (unless electric space heating and cooling are dominant). Second, the influence of the total floor area on electricity consumption is stronger in a large family, since the number of occupied rooms and energy use for lighting, heating, and cooling increases with the number of family members. Finally, for the same floor area and household size, the electricity consumption in a detached house is greater than that of an apartment.

MODELLING PROCEDURE

Dataset

Thirteen months’ (January 2014 – January 2015) data from a grid-connected PV system installed on the grid-connected rooftop of 287 detached residential dwelling located in the Tokyo area is considered. Figure 2 displays the weekly averaged

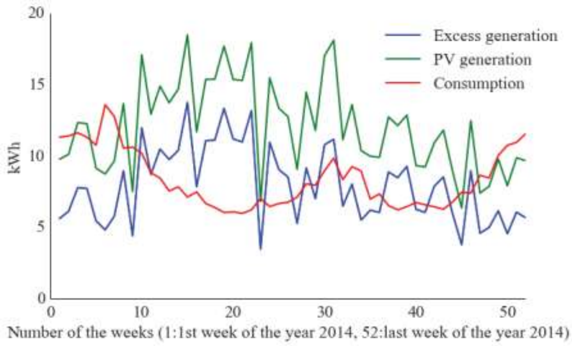

Figure 2: Averaged weekly energy dataset of all households from 1st January to 31st December 2014.

energy dataset over all sampled households: excess-generation and PV generation have peaked during the spring to summer (around week 15-32) except rainy season (week 20-25), whereas electricity consumption has dual peaks in the summer and winter. The dataset has been strictly anonymised.
In addition to monitored energy data, some parameters found useful upon reviewing existing models are collected via questionnaires. These include panel characteristics (angle, azimuth and capacity), number of people living in a household, floor area (m^2), and heating source (gas-heating/all electric). Some households are all-electric dwellings, using only electric power for heating and domestic hot water, cooking equipment, etc. This means the entire energy consumption of such dwellings is recorded using only the electricity monitors.

Metered energy dataset, PV generation, consumption, and excess-generation, are aggregated over daytime (6am to 6pm) since only daytime energy activities should be considered for this purpose: G_d(daytime PV generation), C_d (daytime consumption), and E_d(daytime excess generation).

The list of available explanatory variables per household used in this analysis is shown in Table 1.

One important note is that near-time value of energy dataset by itself is not appropriate to utilise as an explanatory variable as it is unavailable for future prediction. However, aggregated value over a time-period T might be fair to add if T is long enough since these values are inferable from similar sites within the region, or from historical data. In this computation, period T is set as January 2014 to December 2014.

The dataset used in this study is classified into two types of data: the explanatory variables and the objective variable. The objective variable is always excess-generation E_d in this paper, and the explanatory variables are described in Table 1. The importance of these variables will be investigated for model development.

Table 1
List of explanatory variables

VARIABLE	DESCRIPTION
W_{house}	Sum of panel capacity in a house
AZ_{house}	Largest panel's azimuth in a house
AN_{house}	Largest panel's angle in a house
$C_{T,Mean}$	Average of C_T(Set of C_d over the period *T*)
DNR_T	Daytime/Night-time ratio over the period T
$E_{T,Mean}$	Mean of E_d over the period T
$E_{T,Max}$	Max of E_d over the period T
$E_{T,STD}$	Standard deviation of E_d over the period T
E_{d-j}	Historical excess-generation before j day (*j* =1,2,3,7)
E_{system}	Heating system (0: gas heating, 1: all electric)
N_{people}	Number of people in a house: from 1to 7
n_{day}	Number of day
m	Month
$Week$	Week
La	Latitude
Lo	Longitude
S_{floor}	Floor area
$t_{d,ave}$	Average of daily air temperature (Celsius)
$t_{d,max}$	Daily maximum temperature (Celsius)
$t_{d,min}$	Daily minimum temperature (Celsius)
h_d	Daily Humidity (Percentage)
Pr_d	Daily Precipitation (mm)
v_d	Daily Wind velocity (m/s)
I_d	Daily Insolation (kWh)

To evaluate the performance of modelling, this dataset is split into two groups: a training dataset and an evaluating dataset. The datasets are grouped by each month for monthly comparison:

$$\mathbf{D}_m = \{\{\mathbf{x}_m, \mathbf{y}_m\} | m = 1,2,\cdots 13\} \quad (1)$$

where, m is the month of dataset starting from January 2014, and m=13 is the January 2015.

Model Selection

In order to quantify uncertainty in excess-generation predictions, this paper uses a Gaussian Process (GP) model (Rasmussen and Williams 2006) for an excess-generation modelling framework. Traditional linear regression models are easier to implement but pose two major drawbacks: First, they assume (linear) relationship between independent and dependent variables. As a result, they do not capture complex nonlinear behaviour of excess generation and multivariable interactions among variables. Second, they assume constant variance of predictions throughout the entire range of observations, which implicitly requires large data sets to ensure the prediction reliability. Unlike the traditional linear models, a GP model does not require specification of the structural relationship between independent and dependent variables, and consequently they can capture complex behaviour with fewer parameters. In addition, as the parameters of the GP model are trained under a Bayesian setting, the resulting model naturally allows quantification of uncertainties in prediction. (Heo et al., 2012) demonstrated the strengths of the GP model to predict energy use in comparison to the linear model.

GP is a collection of random variables, any finite number of which has Gaussian distributions (Rasmussen, 2006). GP is specified by a mean function $m(\mathbf{x})$ and covariance function $k(\mathbf{x}_i, \mathbf{x}_j)$. A mean function is a matrix of mean output values for the given set of input values. Typically, the mean function $m(\mathbf{x})$ is assumed to be zero. The covariance function $k(\mathbf{x}_i, \mathbf{x}_j)$ used in this analysis is defined in Equation (2). The covariance matrix quantifies proximity between two sets of input values with respect to their outputs. We used a squared exponential function, which is appropriate for modelling very smooth functions.

$$k(\mathbf{x}_i, \mathbf{x}_j) = \theta_0 \exp\{-\frac{1}{2\gamma^2}||\mathbf{x}_i - \mathbf{x}_j||^2\} + \theta_1 \quad (2)$$

where $\theta = (\theta_0, \theta_1, \gamma)$ are hyper parameters, each of which denotes signal variance factor, noise variance factor, and length scale factor, respectively. Those hyper-parameter values are trained to maximise the fit between predictions and observations through a log likelihood function of $\log P(\mathbf{y}|\theta)$ given by

$$\log P(\mathbf{y}|\theta) = -\frac{1}{2}\{\log(\mathbf{K}(\mathbf{X},\mathbf{X}) - \mathbf{y}^T\mathbf{K}(\mathbf{X},\mathbf{X})^{-1}\mathbf{y} - n\log(2\pi)\} \quad (3)$$

where $\mathbf{y}$ denotes observations on the output (excess generation in our study) at known conditions x (e.g., all the explanatory variables in Table 1) and $\mathbf{K}$ is covariance matrix for given set of input values $\mathbf{X}$. With the optimal hyper parameters θ^* derived from training, the mean vector $\boldsymbol{\mu}_{\mathbf{pred}}$ and the covariance matrix $\mathbf{V}_{pred}$ to yield probabilistic outputs for new input values $\mathbf{X}^*$ are given by

$$\boldsymbol{\mu}_{\mathbf{pred}} = \mathbf{K}(\mathbf{X}^*,\mathbf{X})^{\mathrm{T}}\mathbf{K}(\mathbf{X},\mathbf{X})^{-1}\mathbf{y} \quad (4)$$

$$\mathbf{V}_{pred} = \mathbf{K}(\mathbf{X}^*,\mathbf{X}^*) - \mathbf{K}(\mathbf{X}^*,\mathbf{X})^{\mathrm{T}}\mathbf{K}(\mathbf{X},\mathbf{X})^{-1}\mathbf{K}(\mathbf{X},\mathbf{X}^*) \quad (5)$$

For model validation, the dataset is randomly split into two subsets based on a commonly considered rule: 70% for training and 30% for test. With the test dataset, we compare predictions with actual observations with use of MSE (mean squared error) defined in Equation (6).

$$\mathrm{MSE} = \frac{\sum_{i=1}^{n}(\mathbf{y}^*(i) - \boldsymbol{\mu}_{\mathbf{pred}}(i))^2}{n} \quad (6)$$

Table 2
List of feature clusters (FC)

CLUSTER	DESCRIPTION	FEATURES
FC 1	Panel attribute (static)	W_{house} AZ_{house} AN_{house} $Cell_{house}$
FC 2	Household characteristic (static)	N_{people} S_{floor} E_{system}
FC 3	Geospatial information	La Lo
FC 4	Time information	m $Week$ n_{day}
FC 5	Meteorological information	$t_{d,ave}$ $t_{d,max}$ $t_{d,min}$ h_d Pr_d v_d I_d
FC 6	Consumption indicators	DNR_T $C_{T,Mean}$
FC 7	Excess-generation aggregation	$E_{T,Max}$ $E_{T,Mean}$ $E_{T,STD}$
FC 8	Historical dataset	E_{d-1} E_{d-2} E_{d-3} E_{d-7}

where $\mathbf{y}^*$ is the metered excess-generation, $\boldsymbol{\mu}_{\mathbf{pred}}$ is the predicted excess-generation, and n is the number of data in the test dataset.

Feature Selection

Correlation analyses are performed to identify relative importance of PV generation and on-site consumption on excess generation. All data points in 2014 are used. The pearson correlation values are 0.93 with PV generation, and -0.29 with consumption. These results show that PV generation has a strong correlation while on-site consumption has a weak correlation, and it is visible in Figure 2.

We identified twenty-seven potential explanatory variables for model development (Table 1), which can be grouped into eight feature clusters (FC) in order of sampling cost (Table 2); Accordingly, static features (FC 1-4) come first, followed by time-varying features such as meteorological information (FC 5) and historical energy consumption/generation (FC 6-8). Consumption related parameters, average daytime consumption and daytime/night-time ratio over time *T,* are grouped within FC 6. Aggregated values of historical excess generation over time *T* are grouped within FC 7. FC 8 includes near-time excess generation; For example, $E_{d\text{-}1}$ is previous day's excess generation.

Model Development

In a model development, identifying an optimum set of key features is vital to ensure forecasting accuracy while minimizing the cost of data collection. Required computation power is also greatly reduced as the number of explanatory

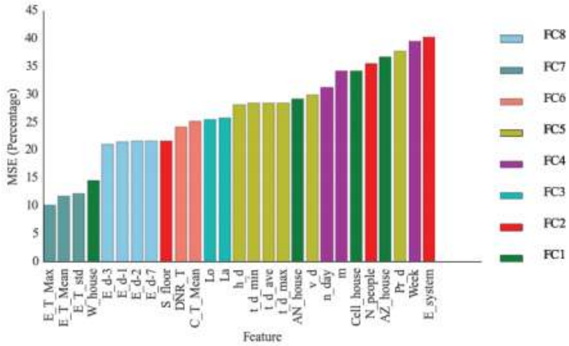

Figure 3: Model accuracy trained with a single variable and sorted in order of MSE score (colour represents FC).

variables becomes smaller. This section describes the process followed in this project to identify an optimum set of explanatory (input) variables for the GP model.

First, individual feature effect on the model accuracy is examined by adding one parameter at a time.

As solar insolation is well-acknowledged as an important parameter that determines PV generation and consequently excess-generation, solar insolation I_d is selected as the primary feature, and all other features listed in Table 2 are subsequently added one at a time. Figure 3 plots the relative influence of all features in order of MSE.

Overall, most features within the same cluster shows similar effect on prediction accuracy, as it is visualised in different colours in Figure 3. Aggregated historical excess-generation features under FC 7 are the top three (MSE value of 10), followed by panel capacity (W_{house}) and the four FC 8 features. The lowest MSE value was achieved by insolation I_d and historical value of maximum daily excess generation over the period *T*: $E_{T,Max}$.

As the second step, all features are added incrementally in order of their corresponding MSE values to determine the optimal number of key explanatory variables to be included in the model. In this sequential analysis process, only features that achieved more than 1% of MSE improvement are considered. As the outcome of this sequential process ,I_d ,E_{d-1},$E_{T,Max}$,$t_{d,min}$ are the four features that best explain excess generation. This experiment clearly shows the importance of analysing model features collectively, as it enables removing important but redundant variables. For the modelling purpose, static parameters such as number of occupants do not explain excess generation.

Finally, the accuracy of the model with these four features is examined by comparing the prediction

Table 3
Result comparison of the model

INPPUT FEATURES	MSE
$I_d E_{d-1} E_{T,Mean}\ t_{d,min}$	9.032
All 28 features	8.212

accuracy of the model with the four features only against a model with all the features as input variables. Table 3 shows that the model with the top four features produces a competitive level of accuracy in comparison to using all the features as input variables.

MODEL VALIDATION

The developed model is validated against unseen evaluation dataset $\mathbf{D}_{eval}$.

From the entire dataset, $\mathbf{D}_{train}$ is a training dataset starting from January 2014 to $m-1$ month, while $\mathbf{D}_{eval}$ is the evaluation dataset starting from month m, as defined in Equation (7) and (8). As an increase of m, the model trained with longer training period is expected to have better extrapolation for an unseen evaluation dataset.

$$\mathbf{D}_{train} = \left\{ \sum_{N=1}^{m-1} \mathbf{D}_m \,\middle|\, m = 2,3,\cdots 13 \right\} \tag{7}$$

$$\mathbf{D}_{eval} = \left\{ \sum_{N=m}^{13} \mathbf{D}_m \,\middle|\, m = 2,3,\cdots 13 \right\} \tag{8}$$

Decoupled Model Description

As described in the introduction, excess generation can be decoupled into two energy components: PV generation and on-site consumption. Hence, it is natural to think that two individual energy models can substitute an integrated excess-generation model. In theory, the exact daily aggregated value of excess PV generation can be expressed as:

$$\boldsymbol{E}_d^{integrated} = \sum_{day} \max(g(t) - c(t), 0) \tag{9}$$

where *g(t)* and *c(t)* are respectively the generation and consumption at time t.

When we approximate excess PV generation by separately aggregating daily consumption and generation, we however end up estimating excess generation as:

$$\boldsymbol{E}_d^{decoupled} = \max(G_d - C_d, 0) \tag{10}$$

where $\boldsymbol{G}_d = \sum_{day} g(t)$ and $\boldsymbol{C}_d = \sum_{day} c(t)$.

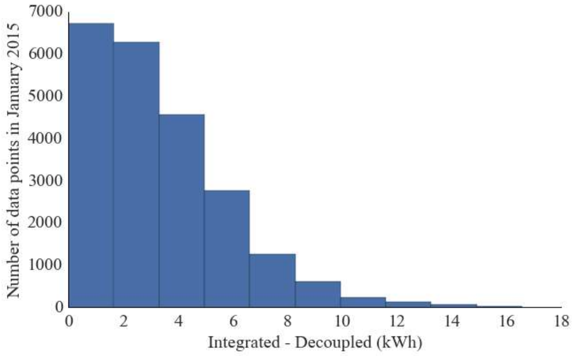

Figure 4: Error distribution of $(E_d^{integrated} - E_d^{decoupled})$ *in January 2015.*

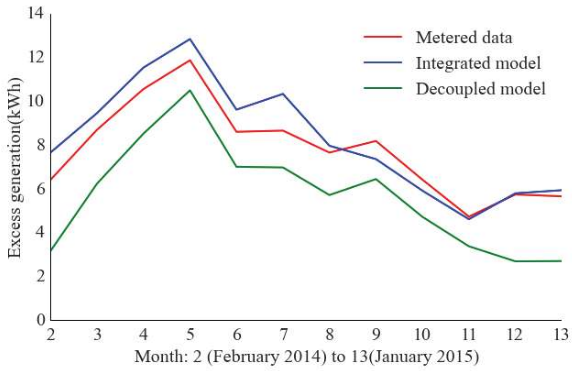

Figure 5: Monthly scale of forecasting results against metered data from January 2014 to January 2015.

We notice that $E_d^{integrated} \geq E_d^{decoupled}$ if *g(t)* is smaller than *c(t)* any time: hourly electricity demand is higher than hourly on-site generation. If no aggregation over a daily time duration is performed, the decoupled approach can properly predict hourly excess-generation.

However, if consumption and generation values are aggregated over any duration, the decoupled approach is most likely to underestimate the true value of excess-generation by subtracting some electricity demands, met by the grid supply, from the aggregated on-site generation.

Figure 4 represents the distribution of the discrepancy between the integrated and decoupled approaches ($E_d^{integrated} - E_d^{decoupled}$). This figure confirms the concerned discrepancy happens frequently causing more than 2kWh differences. This illustrates the unavoidable nature of underestimation in the decoupled approach: excess-generation is highly likely larger than the value obtained from a decoupled approach if the values are aggregated over any duration.

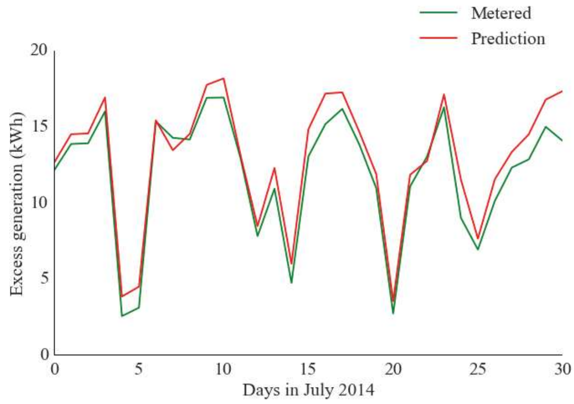

Figure 6: Daily scale of forecasting results against metered data in July 2014 (overestimated example).

Prediction results

Prediction results by the proposed integrated excess-generation models are compared against both metered data and the values obtained from the decoupled approach. In the decoupled model, metered daytime (6:00 to 18:00) aggregated values of PV generation and consumption are used, instead of modelling them individually. This means that the values used removes inaccuracy of these models and uncertainties of model parameters, and represents the most accurate values.

Figure 5 displays the excess-generation predicted by the integrated excess-generation model and the decoupled model against true values of excess generation (metered data). This shows that the decoupled approach tends to consistently underestimate the exact value of excess generation, and this phenomenon is remarkable during the winter seasons. This result confirms the previous mathematical examination on the drawback of the decoupled approach, and, therefore, elucidates the necessity of development of tailored excess-generation modelling.

Lengths of the training period

As shown in Figure 5, the integrated excess-generation model tends to overestimate in peak generation periods during spring and summer seasons, and prediction error is noticeably low during the autumn and winter seasons. Whether the model adjusts its tendency of overestimation to slight underestimation by learning from more datasets, or the model itself has a tendency to overestimate in peak generation, and underestimate in off-peak generation, is yet to be analysed.

For further examination, the forecasting results are illustrated at daily resolution. Figure 6 and Figure 7 displays two distinctive months. These figures confirm that the model successfully followed the fluctuation of excess-generation closely in daily

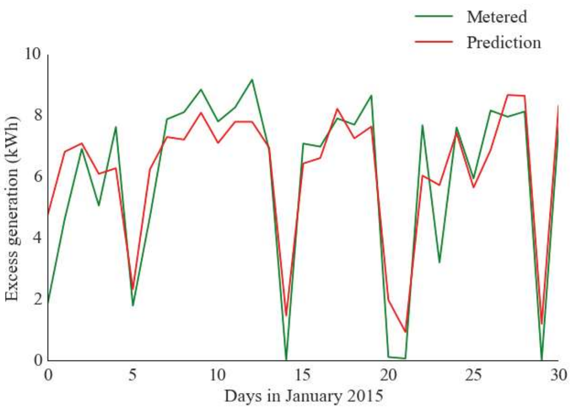

Figure 7: Daily scale of forecasting results against metered data in January 2015 (underestimated example).

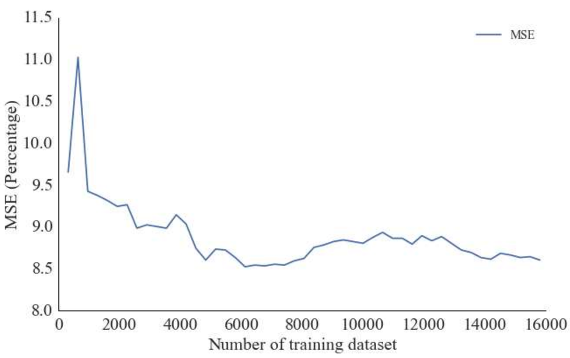

Figure 8: Effect of the number of data point on the model accuracy. Each data point represents a day of a household.

basis. In Figure 6, the prediction is constantly overestimated, whilst in Figure 7 the tendency is adjusted mostly. This leads to a conclusion that the model modified its initial overestimation tendency, by learning from different seasonal dataset. Hence, this paper reconfirms the importance of a-year-long minimum data collection in a single site, with multiple distinct seasons.

Effect of the number of training points

The biggest barrier for the development of such a data-driven model is the cost incurred in collecting actual energy data from residential households for a-year-long period. The time complexity is also a factor; a GP has cubic time (n^3), where n is the number of training data points. Hence, minimising the size of the training dataset has vital importance for realistic implementation. In this section, the consequence of the number of training points on the performance of the model is analysed. To do so, we consider limited data points randomly chosen from all data points and the result is plotted in Figure 8.

In the range of 6,000-16,000 points, the MSE changes are always within the same order of magnitude. If the number of data points is reduced below 6,000, the MSE increases significantly. The outcomes indicate the model seems to converge by 6,000 data points.

This trial points out that 6,000 data points is the optimal amount of training data necessary to accomplish the best performance with the least computation cost. If 365 data points can be collected per a household for a-year long survey, 6,000 data points is equivalent to 18 households. This number sounds realistic to reproduce this trial anywhere in the world.

CONCLUSION AND FUTURE WORK

To the best of the author's knowledge, this paper proposed the first integrated data-driven GP model for daily excess electricity generation. The analysis present a framework to develop a GP model by identifying effective features, and demonstrates a way to minimise the number of necessary datasets without compromising predictive accuracy.

This paper demonstrates how to optimise required set of features, training data periods and number of households, which directly link to cost of data collection and computational power. Four features, two of historical excess-generation data and two of weather parameters, are shown to be effective combination. Also, a-year long data collection from 18 households produces the optimal number of training datasets for robustness against seasonality.

This research also reveals a particular drawback of the decoupled approach to quantify excess-generation. The proposed model presents much higher prediction performance than the decoupled value (daytime generation minus daytime consumption), which has unavoidable tendency of significant underestimation. It reaffirms the necessity of excess-generation model.

One scheduled further work is to develop a model of household behavioural adoption under TOU-based financial incentives. FIT is a kind of TOU tariffs, which incentivises lower energy consumption in daytime. Currently FIT prices are currently much higher (38-42 JPY per kWh) than the average electricity bill (20-25 JPY per kWh) (METI., 2012), so customers have a strong financial incentive to maximise their excess-generation. PV-owned households presumably have changed their behaviour by shifting electricity-heavy appliances, such as dishwashers and washing machines, to evening use. (Torriti., 2012) confirmed in a two-year study that financial incentives such as time-of-use (TOU) cause a significant level of load shifting. Such a behavioural adoption has not been considered in this paper. In order to do so, the model presented in this paper will be adapted to a shorter time resolution that corresponds to activities associated with electricity consumption in households.

REFERENCES

Clean Energy Decision Support Centre. 2004. RETScreen ® International CLEAN ENERGY PROJECT ANALYSIS.

Denholm, P., Robert M. M. 2007. Evaluating the Limits of Solar Photovoltaics (PV) in Electric Power Systems Utilizing Energy Storage and Other Enabling Technologies, *Energy Policy*.

Huang, Y., Lu, J., Liu, C., Xu, X., Wang, W., Zhou, X. 2010. Comparative Study of Power Forecasting Methods for PV Stations, Hangzhou, China.

Heo, Y., Zavala, V. M., 2012. Gaussian process modelling for measurement and verification of building energy savings, *Energy and Buildings*.

IEA. 2010., Technology Roadmap: Solar Photovoltaic Energy, May, IEA Technology Roadmaps, OECD Publishing.

Jayanta, D. M., Yigzaw, G. Y., Brian, N., 2007., Comparison of measured and predicted long term performance of grid a connected photovoltaic system, *Energy Conversion and Management*.

Long, H., Zhang, Z., Su, Y., 2014. Analysis of daily solar power prediction with data-driven approaches, *Applied Energy*.

METI. 2012. FEED-IN TARIFF SCHEME IN JAPAN.

Pinson, P., Chevallier, C., Kariniotakis, G. N. 2007. Trading wind generation from short-term probabilistic forecasts of wind power, *IEEE Transaction on Power Systems*.

Parti, M. 1980. The Total and Appliance-Specific Conditional Demand for Electricity in the Household Sector, *The Bell Journal of Economics*.

Rasmussen, Carl, E., Christopher, K. I. W. 2006. Gaussian Processes for Machine Learning, *MIT Press*.

Shimoda, Y., Takahiro, A., Ayako, T., Minoru, M. 2007. Evaluation of City-Scale Impact of Residential Energy Conservation Measures Using the Detailed End-Use Simulation Model. *Energy*.

Shimoda, Y., Takuro F., Takao M., Minoru M. 2004. Residential End-Use Energy Simulation at City Scale, *Building and Environment*.

Türk, T., Inci, Emin, O. 1999. A Study for Estimating Solar Radiation in Elaziğ Using Geographical and Meteorological Data, *Energy Conversion and Management*.

Torriti, J. 2012. Price-based demand side management: Assessing the impacts of time-of-use tariffs on residential electricity demand and peak shifting in Northern Italy, *Energy*.